

A brief review of “solar flare effects” on the ionosphere

B. T. Tsurutani,¹ O. P. Verkhoglyadova,^{1,2} A. J. Mannucci,¹ G. S. Lakhina,³ G. Li,^{2,4} and G. P. Zank^{2,4}

Received 7 October 2008; revised 29 January 2009; accepted 6 May 2009; published 25 July 2009.

[1] The study of solar flare effects (SFEs) on the ionosphere is having a renaissance. The development of GPS ground and satellite data for scientific use has opened up new means for high time resolution research on SFEs. At present, without continuous flare photon spectra (X rays, EUV, UV, and visible) monitoring instrumentation, the best way to model flare spectral changes within a flare is through ionospheric GPS studies. Flare EUV photons can increase the total electron content of the subsolar ionosphere by up to 30% in ~ 5 min. Energetic particles (ions) of 10 keV to GeV energies are accelerated at the flare site. Electrons with energies up to several MeV are also created. A coronal mass ejection (CME) is launched from the Sun at the time of the flare. Fast interplanetary CMEs (ICMEs) have upstream shocks which accelerate ions to ~ 10 keV to ~ 10 MeV. Both sources of particles, when magnetically connected to the Earth’s magnetosphere, enter the magnetosphere and the high-latitude and midlatitude ionosphere. Those particles that precipitate into the ionosphere cause rapid increases in the polar atmospheric ionization, disruption of transpolar communication, and cause ozone destruction. Complicating the picture, when the ICME reaches the magnetosphere ~ 1 to 4 days later, shock compression of the magnetosphere energizes preexisting 10–100 keV magnetospheric electrons and ions, causing precipitation into the dayside auroral zone ($\sim 60^\circ$ – 65° MLAT) ionospheres. Shock compression can also trigger supersubstorms in the magnetotail with concomitant energetic particle precipitation into the nightside auroral zones. If the interplanetary sheath or ICME magnetic fields are southwardly directed and last for several hours, a geomagnetic storm will result. A magnetic storm is characterized by the formation of an unstable ring current with energetic particles in the range ~ 10 keV to ~ 500 keV. The ring current decays away by precipitation into the middle latitude ionosphere over timescales of ~ 10 h. A schematic of a time line for the above SFE ionospheric effects is provided. Descriptions of where in the ionosphere and in what time sequence is provided in the body of the text. Much of the terminology presently in use describing solar, interplanetary, magnetospheric, and ionospheric SFE-related phenomena are dated. We suggest physics-based terms be used in the future.

Citation: Tsurutani, B. T., O. P. Verkhoglyadova, A. J. Mannucci, G. S. Lakhina, G. Li, and G. P. Zank (2009), A brief review of “solar flare effects” on the ionosphere, *Radio Sci.*, 44, RS0A17, doi:10.1029/2008RS004029.

1. Introduction

[2] Enhanced X-ray fluxes during solar flares are known to cause increased ionization in the Earth’s lower

ionosphere (*D* region). This alteration of the ionospheric electron density profile, called a sudden ionospheric disturbance (SID), is deleterious to radio wave communication and navigation. Although such solar flare effects (SFEs) on the Earth’s ionosphere have been known for many decades [Thome and Wagner, 1971; Mitra, 1974; Donnelly, 1976] (we refer the reader to Pröls [2004], for a comprehensive review), these past studies are recognized as being rudimentary in comparison to what is now possible. SFE flare studies have been greatly aided by the new technology of GPS ground and satellite receivers [Klobuchar, 1997; Afraimovich, 2000; Zhang *et al.*, 2002]. The thousands of ground receivers can be used to

¹Jet Propulsion Laboratory, California Institute of Technology, Pasadena, California, USA.

²CSPAR, University of Alabama, Huntsville, Alabama, USA.

³Indian Institute of Geomagnetism, Navi Mumbai, India.

⁴Department of Physics, University of Alabama, Huntsville, Alabama, USA.

Table 1. Characteristics of Particle Populations in the Interplanetary Space From the Sun to 1 AU

Particle Populations	Energy Range
GCR	GeV–TeV
Anomalous CRs	10–00 MeV
SEPs	10 keV–GeV
ESP particles	keV–100 MeV

obtain high time resolution (~ 30 s) and high spatial resolution global changes in the dayside total electron content (TEC). Satellite occultation data can obtain vertical cuts through the ionosphere yielding the height dependence of the enhanced ionization. The combined data sets could be inverted to determine the solar flare spectra as a function of time (such detailed solar measurements are unfortunately not available at present).

[3] Recently, *Tsurutani et al.* [2005] studied the ionospheric effects of the intense solar flares of 28 and 29 October and 4 November 2003 (the “Halloween” events) and 14 July 2000 (Bastille Day event) using both spacecraft data (SOHO, GEOS, TIMED) and ground-based GPS receiver data. The flare locations were: $S18^\circ E20^\circ$, $S19^\circ W09^\circ$, $S18^\circ W88^\circ$, and $22^\circ N 07^\circ W$, respectively (courtesy of NOAA). The largest impact on the dayside ionosphere (a ~ 25 TECU peak increase, where a TECU = 10^{16} electron m^{-2}) was the 28 October 2003 solar flare (X17) and not the more intense X-ray flare of 4 November 2003 (X28). The latter event caused only a moderate ~ 5 – 7 TECU increase. Since the 28 October solar flare EUV peak flux increase was double that of the 4 November flare, it was concluded that the solar EUV flux was primarily responsible for the increased TEC in the ionospheric *E* and *F* regions during and immediately after solar flares. This study emphasized the importance of the spectra of solar flares for SFES. *Dmitriev et al.* [2006] studied the response of the ionosphere to X-ray emissions and solar energetic particles during the above solar flares. *Sahai et al.* [2006] noted unusual Brazilian sector ionospheric effects associated with the 28 October flare.

[4] Another type of SFES are associated with energetic particles with energies from several 10 keV up to several 100 MeV and higher. Sources of these particles are solar energetic particles (SEPs) accelerated at the flare site, presumably by magnetic reconnection [*Cohen*, 1976; *Litvinenko*, 2003] and other processes such as wave-particle interactions [*Miller et al.*, 1996], and particles accelerated at ICME shocks called energetic storm particles (ESPs). There is a clear distinction between different populations which are specified according to particle origin or acceleration region (see Table 1 and reviews by *Kallenrode* [2001, 2003]). Review on space weather consequences of these energetic particles and prediction models can be found in the work of *Feynman and Gabriel*

[2000]. A brief summary of the particle energies is given in Table 1.

2. Results

2.1. Solar Flare Photon Intensities and Spectra

[5] Figure 1 shows the intense solar flares on 28 and 29 October and 4 November 2003 (the “Halloween” events) and the 14 July 2000 (the “Bastille day”) event. The flares have fast rise and exponential decay flux features located at the center of Figure 1. The data shown are the SOHO SEM 26 to 34 nm wavelength EUV data [*Judge*, 1998]. Because this channel is narrow-banded, it was not saturated during any of the four intense solar flares.

[6] The peak flare intensities given by the NOAA Data Center are: X17, X10 and X28, and X6, respectively. This classification scheme uses a logarithmic (base 10) scale to denote the peak X-ray fluxes in the 0.1–0.8 nm channel of the NOAA GOES instrument. For people who wish to use these data for quantitative studies, several important points should be noted. For the two most intense flares (28 October and 4 November 2003) the X-ray instrumentation became (count rate) saturated. The peak fluxes were estimated by extrapolation. Thus, there may be errors in taking these numbers literally. For example, *Thomson et al.* [2004] have estimated (using an indirect technique) that the 4 November 2003 flare had a much higher intensity of $X45 \pm 5$!

[7] A second feature in Figure 1 is that the flares have variable EUV backgrounds [see *Tsurutani et al.*, 2005, 2006]. Therefore the background should be subtracted out by researchers doing quantitative studies. If the backgrounds are not taken into account, the 4 November 2003 flare event was actually the lowest of all four events in the 26–34 nm bandwidth range.

[8] A third point of interest in Figure 1 is when the preflare background is subtracted out, the 28 October flare is the largest event in EUV by a factor of ~ 2 . Thus if the 4 November 2003 flare is indeed the largest event in 0.1–0.8 nm X rays, then there is a very strong spectral difference between the two flares. Some of this difference may be due to the 4 November event occurring near the limb of the Sun [*Tsurutani et al.*, 2005]. The EUV emissions which are generated lower in the corona may be absorbed by the solar atmosphere during their propagation to the spacecraft [*Donnelly*, 1976; *Afraimovich et al.*, 2002] (*C. Tranquille et al.*, The Ulysses catalog of solar hard X-ray fluxes, submitted to *Solar Physics*, 2008). However, this does not explain why the 28 October 2003 event had lower peak X-ray fluxes. There must have been some intrinsically strong spectral differences between the two flares.

[9] There is no reason to assume that the spectra for different flares are the same (as is commonly done for

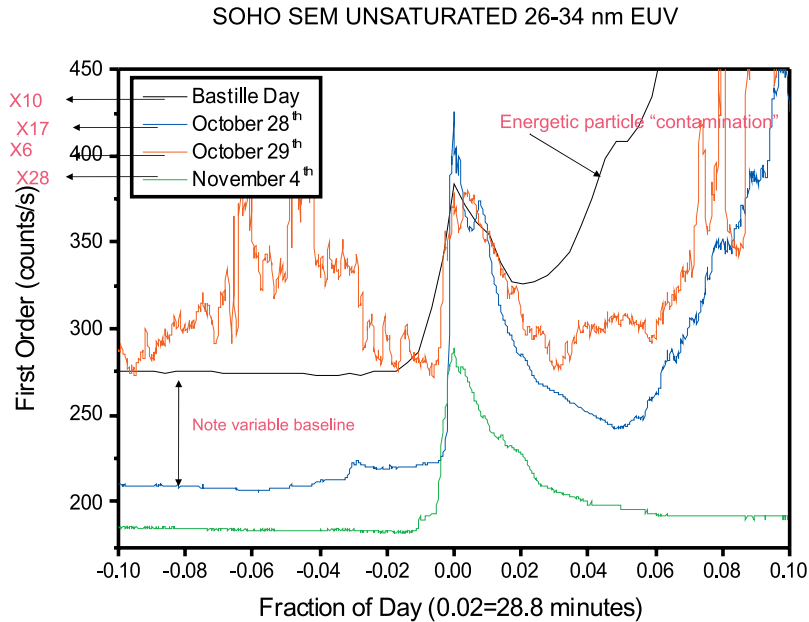


Figure 1. EUV fluxes for the three Halloween 2003 and the Bastille Day solar flares.

modeling purposes). In fact there is strong evidence to the contrary. The stronger the flare is in X-ray flux, usually the steeper the spectrum. Flare X-ray fluxes can vary by 3 or even 4 orders of magnitude, EUV fluxes by much less [Tsurutani *et al.*, 2005; Woods *et al.*, 2004, 2006a, 2006b] and visible light only by a factor of ~ 2 [see Carrington, 1860; Tsurutani *et al.*, 2003a]. The physical cause of this general spectral trend has not been well explained to date.

2.2. Flare Photon Effects on the Ionosphere

[10] Figure 2 shows the ionospheric effects of the 4 November 2003 (Figure 2a) and the 28 October 2003 (Figure 2b) flares. The subsolar point is at the center of Figures 2a and 2b, and local midnight is at the left and right edges. In both cases a two-step background subtraction was performed so that the flare TEC increases can be easily visualized. First, the TEC during the flare was subtracted from the TEC values a few minutes before. This differential TEC (Δ TEC) is computed for the day of the flare and a background day, and then differenced again between the two days to produce Figures 2a and 2b. This double differencing process minimizes contamination from diurnal variability of the ionosphere. In Figure 2a, the background subtraction was applied to 5 November and 4 November. In Figure 2b, the 27 October Δ TEC was subtracted from the 28 October Δ TEC. The 29 October TEC data could not be used as background for this flare event because the ICME associated with the 28 October 2003 flare reached the Earth during this day, causing a large geomagnetic storm [Mannucci *et al.*, 2005]. The

precipitation of the (magnetospheric) storm particles into the ionosphere “contaminated” this latter interval.

[11] The TEC enhancements are noted to occur on the dayside with little or no effects at night, as expected (see discussion of TEC effects near the dawn and dusk terminators in the works of Leonovich *et al.* [2002] and Zhang and Xiao [2003]). The maximum effect of the 4 November event was about ~ 5 to 7 TECU above the background quiet day level. The peak enhancement occurred near the subsolar point. The 28 October peak TEC was much greater, up to ~ 25 TECU about the background day level. It is clear that in EUV wavelengths, the 28 October event was the greater of the two events.

[12] A factor of ~ 2 EUV intensity increase (a ratio of the 28 October to 4 November flux increases) caused a ~ 3 to 4 times difference in ionospheric TECU. Detailed analyses using GPS occultation data can be used to make progress in understanding this apparent discrepancy.

2.3. Energetic Particles Associated With Solar Flares and Interplanetary CMEs

[13] Another important feature in Figure 1 is the count rate increases after the flares have occurred. The event with the largest postflare increase is the 14 July 2000 event, followed by the 29 October 2003 event and then the 28 October 2003 event. The 4 November 2003 event shows little or no postflare increase. These count rate increases are due to solar flare energetic particle contamination of the SOHO SEM detector. The 4 November event was located on the solar limb, so the interplanetary magnetic connectivity between the solar location and the

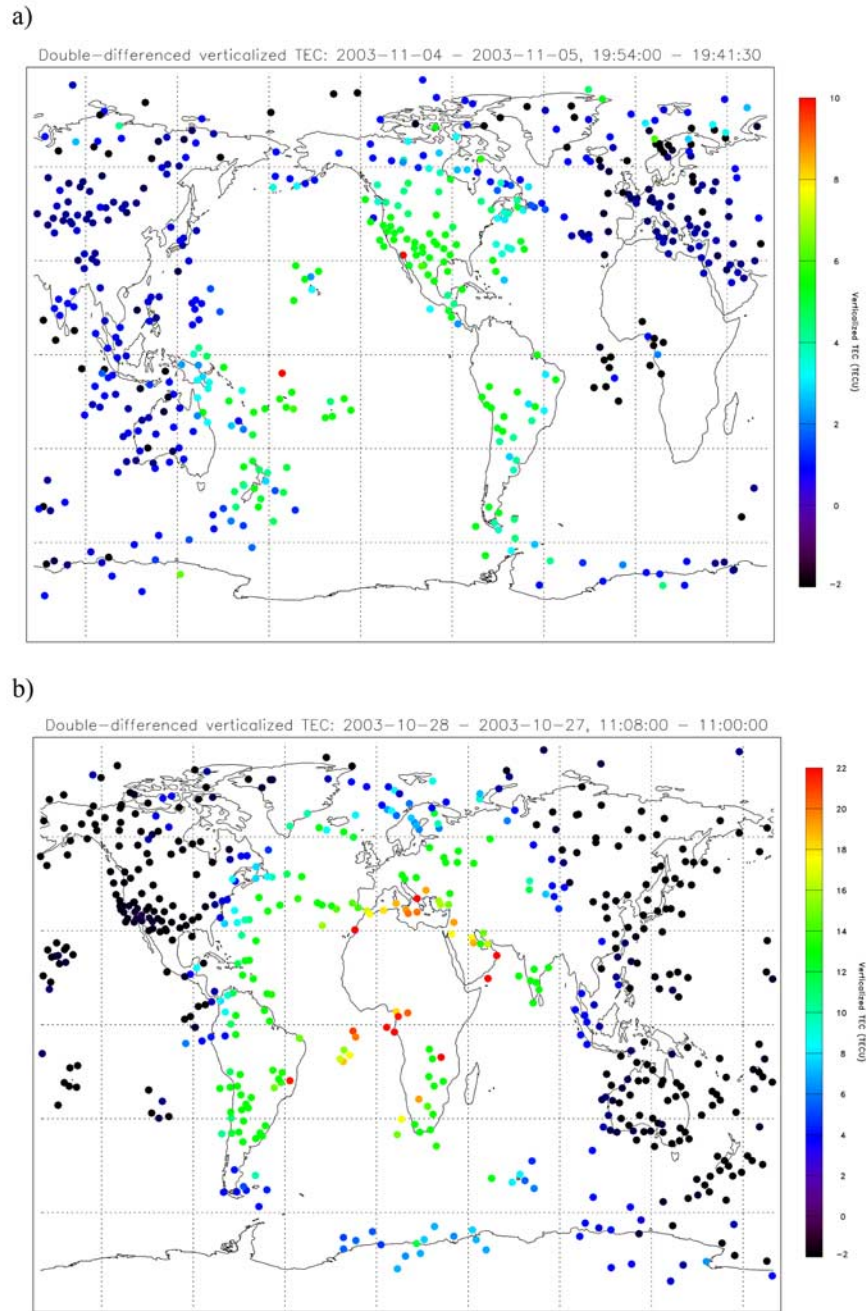


Figure 2. Enhanced ionization for the (a) 4 November 2003 and the (b) 28 October 2003 solar flares. The subsolar points are at the center of the graphs.

Earth was presumably poor and thus the energetic flare particles did not reach the Earth. (The energetic particles are confined to travel along the interplanetary magnetic field lines due to their low-energy densities. These mag-

netic fields map out an Archimedean/Parker spiral due to the rotation of the Sun.)

[14] When the energetic particles reach the Earth, they may penetrate into the Earth's ionosphere. The particles

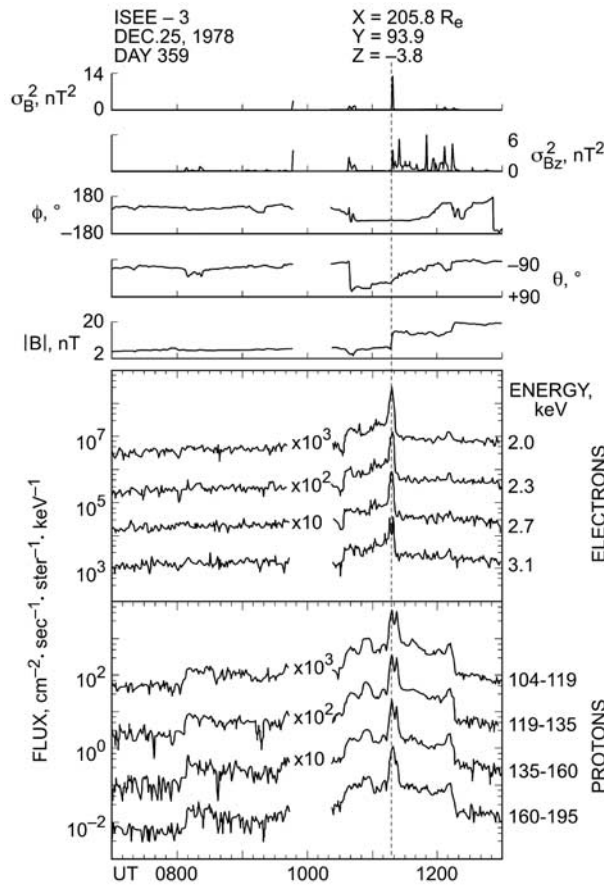


Figure 3. An interplanetary shock detected at 1 AU, $\sim 206 R_e$ upstream of the Earth. The peak flux of energetic electrons and protons are collocated with the fast forward shock. Taken from *Tsurutani and Lin [1985]*.

have easy access to the polar regions of the ionosphere because the Earth’s magnetic field lines are “open.” Particle precipitation in these regions causes polar cap absorptions (PCAs) and radio blackouts. Energetic particles can also reach lower magnetic latitudes depending on their energies and momenta. A rough law of the minimum momentum for proton penetration to the top of the ionosphere is $\sim 15 \text{ GeV} \cos^4 \theta$ where θ is the magnetic latitude [*Fermi, 1950*].

[15] The more energetic the particle, the deeper the penetration into the atmosphere/ionosphere. Solar flare particles lose their energy by ionization of neutral atoms and molecules [*Fermi, 1950*]. Thus the location of enhanced ionization will depend on both the magnetic connectivity to Earth and the spectra of flare particles that reach the Earth. The energetic particles create HO_x and NO_x in the lower atmosphere. Both HO_x and NO_x act as catalysts for ozone destruction (see *Rohen et al. [2005]* for

discussion of ozone destruction during the Halloween 2003 flare particle events).

[16] There are two main sources of “flare energetic particles.” Those that are accelerated at the flare site itself, and those that are accelerated at the interplanetary coronal mass ejection (ICME) forward shock. In the literature, the former have been called Solar Energetic Particle (SEP) events or “prompt particle” events and the ESP events or “delayed particle” events. Although ICME shock particles can be accelerated and released from distances very close to the Sun, greater fluxes are detected as the ICME/shock approaches the Earth. ICMEs and their shocks are much delayed from the flare onset time, taking ~ 1 to 4 days to propagate from the Sun to the Earth.

[17] Figure 3 shows an example of an ICME shock and energetic particles at a spacecraft at ~ 1 AU. The first through the fifth panels are interplanetary magnetic field parameters. The jump in magnetic field magnitude indicates the occurrence of a fast forward shock (denoted by a vertical dashed line) antisunward of the ICME. A full Rankine-Hugoniot analysis of this structure was performed to prove that it was indeed a fast shock. These details have been omitted to conserve space. The sixth and the seventh panels show that energetic 2.0 to 3.1 keV electron and 104 to 195 keV proton peak fluxes are coincident with the shock and are presumably accelerated by the shock.

2.4. Modeling Contributions From Flare and Shock-Accelerated Particles to a SEP Event

[18] The Particle Acceleration and Transport in the Heliosphere (PATH) code has been developed to model radiation environment produced by a SEP event at the Earth orbit [*Zank et al., 2007; Verkhoglyadova et al., 2008a, 2009*]. The PATH code is used to determine relative contributions of flare and solar wind particles and are matched to observed spectra at 1AU for a specific event [see also *Li and Zank, 2005*]. The approach combines input from both flare particles and particles accelerated at an ICME-driven shock. The code traces the shock propagation, model solar wind particle acceleration at the shock and escape from the shock, and transport of particles of the flare and solar wind origin throughout the heliosphere. The models are based on a first-order Fermi mechanism of particle acceleration at a shock, known as a diffusive shock acceleration (DSA) mechanism [*Axford et al., 1977; Bell, 1978*]. The code output are instantaneous and time-averaged spectra at 1 AU, and particle fluxes in a wide energy range. Details of the models are described by *Zank et al. [2000, 2007]*, *Li et al. [2003, 2005]*, and *Verkhoglyadova et al. [2009]*.

[19] The SEP event of 13 December 2006 was associated with an X3.4 class flare. The start of the flare was at 0254 UT as measured by the GOES satellites (Figure 4,

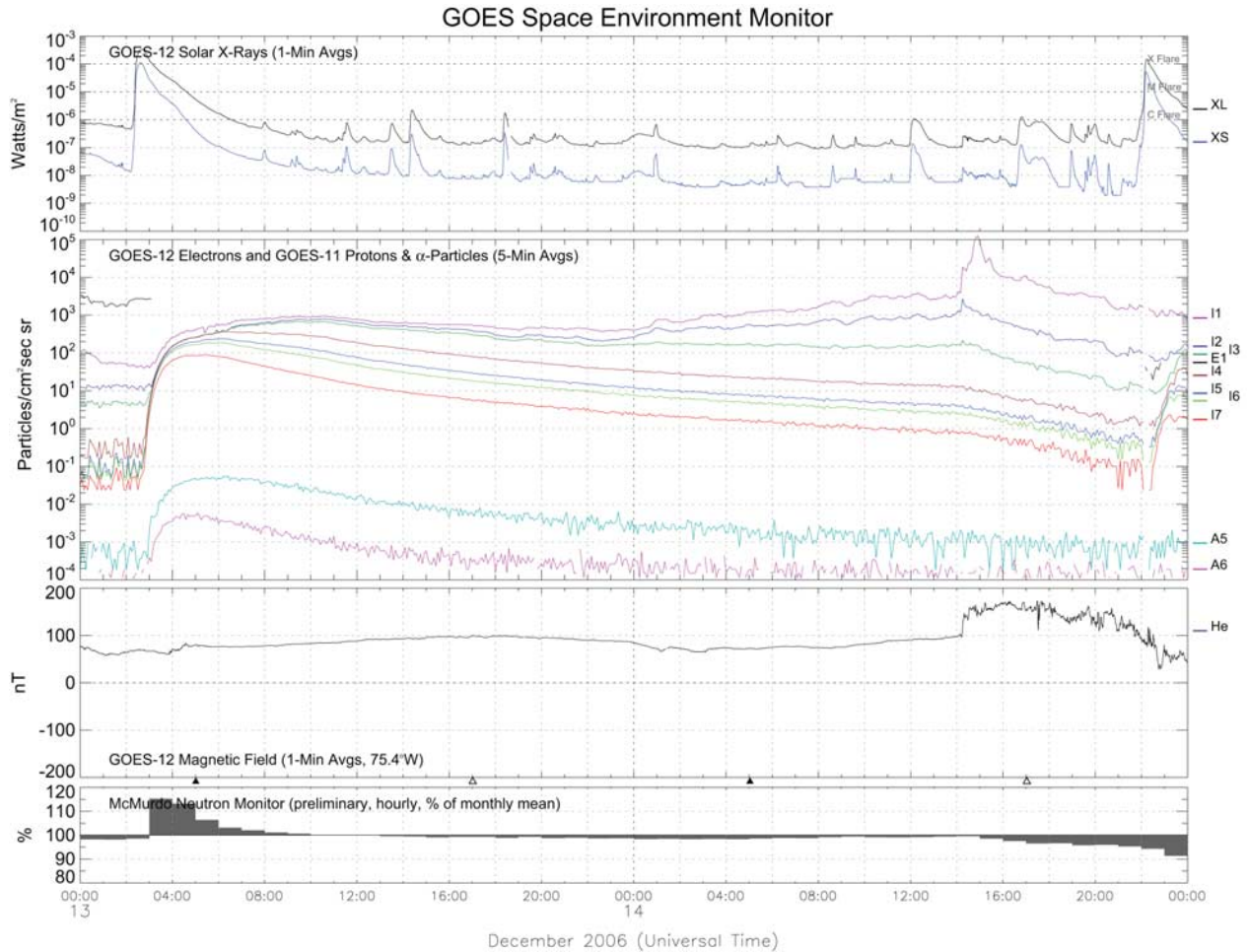


Figure 4. Data from the Earth-orbiting GOES satellite for 13 and 14 December 2006. The X-ray flare occurs at ~ 0400 UT on 13 December (first panel), concomitant particle fluxes (second panel), and cosmic ray background increases (fourth panel). The ICME shock arrived the next day at ~ 1400 UT. Particle flux increases and magnetic field compression are related to the shock arrival to the magnetosphere. Courtesy of the NOAA National Geophysical Data Center.

first panel). A ground-level event (GLE) was detected after a short delay from the flare onset (Figure 4, fourth panel). A halo CME event was observed by SOHO and its radial speed was estimated to be ~ 1770 km/s. The ICME-driven shock reached 1 AU at ~ 1400 UT the next day and the corresponding ESP signatures were observed by near-Earth satellites (Figure 4, third panel). Particle fluxes were enhanced during the flare event and low-energy fluxes reached peak values simultaneously with the time of shock arrival (Figure 4, second panel).

[20] To model this event, we assume that the ICME-driven shock is quasi-parallel at 1 AU. ACE measurements provide an estimate of the shock normal angle (normal to the upstream ambient magnetic field) as $\sim 30^\circ$. Flare particles are injected into the shock in

the energy range up to 1 GeV during the duration of the flare (~ 43 min). Particles from the solar wind population (>10 keV/nucleon) are injected into the shock as well. Given certain conditions (minimum energy cutoff, resonance conditions, etc.), injected particles from both sources (the “seed” population) are accelerated up to ~ 100 MeV/nuc energies due to the DSA mechanism. Escaping particles are scattered in pitch angle as they propagate along the interplanetary magnetic field lines. A Monte-Carlo approach is used to model particle transport between the shock and 1 AU and beyond.

[21] Figure 5 presents modeled fluxes of iron ions (the charge to mass ratio is 14/56) at 1 AU for six representative energies in the high-energy range (from 13 to 140 MeV/n) and the low-energy range (from 42 keV/n to

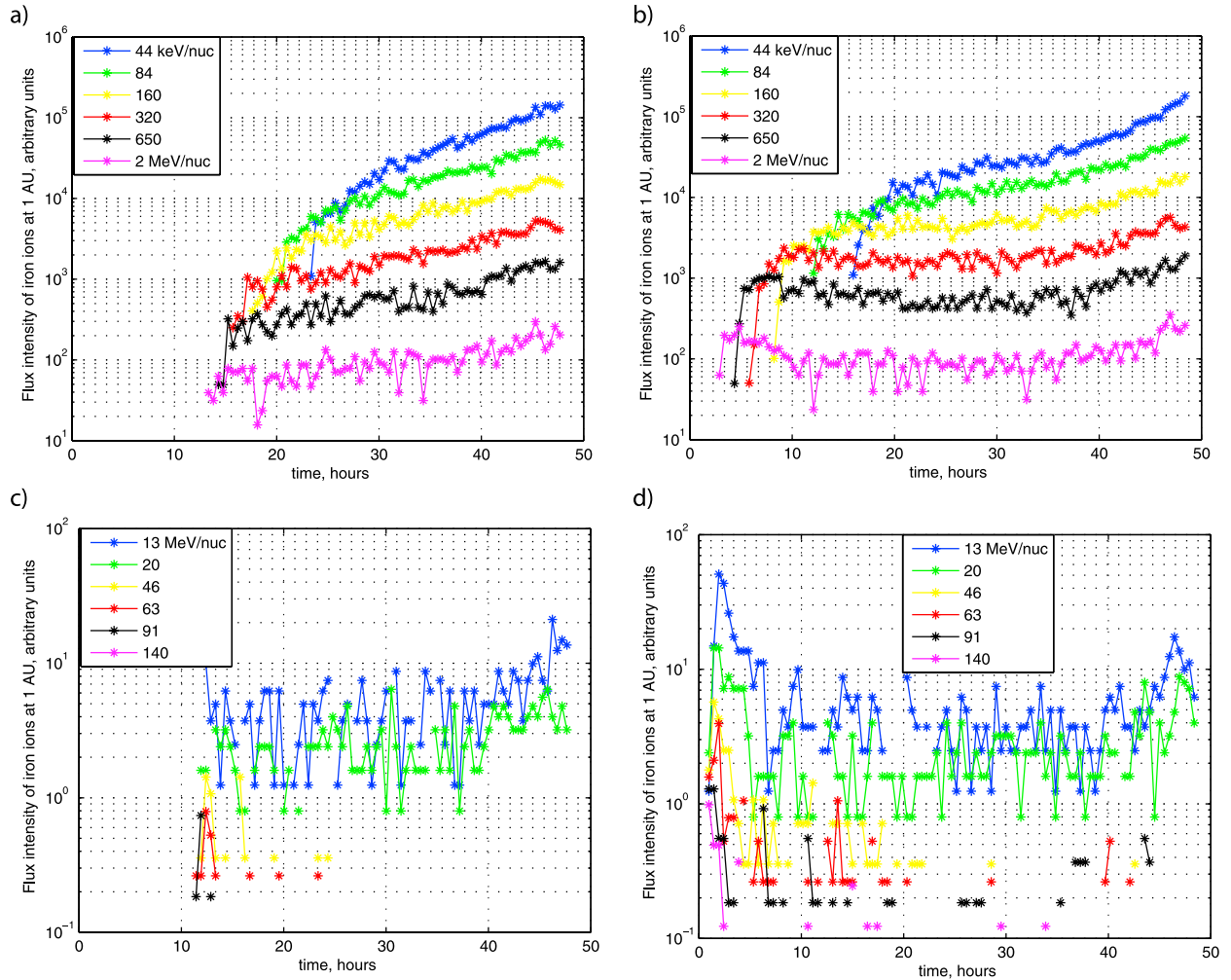


Figure 5. Energetic iron ion flux in (top) six low-energy channels and (bottom) six high-energy channels. (a and c) Results of the PATH model assuming only shock-accelerated particles as the “seeds.” (b and d) Results assuming both flare particles and the shock-accelerated particles as the “seeds.”

2 MeV/n). (These specific energies were chosen because they correspond to instrument energy channels onboard ACE.) We plot fluxes from the moment the shock was launched until its arrival at 1 AU. First, to study shock effects by themselves we run the model without contribution from the flare. The results for fluxes in low- and high-energy ranges are presented in Figures 5a and 5c, respectively. One can notice that high-energy particles arrive first at 1 AU ~ 10 h after the shock initiation near the Sun. Lower-energy particles arrive much later. Contribution from the highest energy particles diminishes with time whereas low-energy particle fluxes increase up to the shock arrival time. A portion of the low-energy particle distribution is trapped behind the shock and has a major impact on the spectrum at the shock arrival time creating

an ESP event. This can explain local maxima observed by SEM/GOES (see Figure 4, particle fluxes) and is reflected in our modeling results (Figures 5a and 5c).

[22] To study cumulative effects from flare particles and the shock-accelerated particles, we run the PATH code from the flare particle input discussed above. Figures 5b and 5d show the sharp rise in the most energetic ions of ~ 100 MeV/nucleon at the beginning of the SEP event. These particles are of the flare origin and contribute to the overall spectrum within the first 5 h. After that, their input decreases. It should be noted that a portion of the flare particles is absorbed by the shock and reaccelerated through the DSA mechanism. Low-energy particles (~ 44 , 84 and 160 keV/nucleon channels) are accelerated at the ICME-driven shock and contribute continuously to

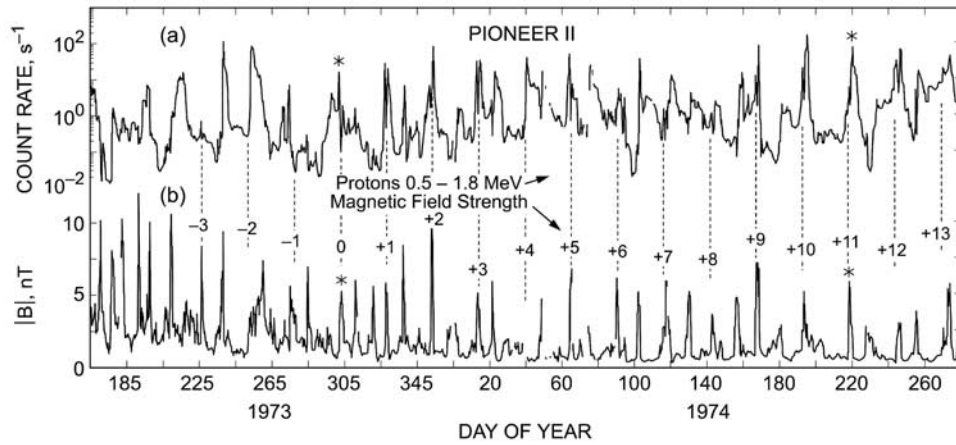


Figure 6. Energetic ~ 1.0 MeV protons accelerated at CIR shocks.

the observed flux. There are distinct peaks corresponding to an ESP event coincident with the shock arrival.

2.5. Corotating Interaction Regions and Energetic Particles

[23] Besides fast ICME shocks, other solar wind features/processes can form shocks that can accelerate energetic particles as well. This third source of energetic particles is not associated with solar flares or with ICMEs. During the declining phase of the solar cycle, high-speed solar wind streams (emanating from coronal holes) run into slower speed streams. The stream-stream interactions form compressed field and plasma regions called Corotating Interaction Regions or CIRs. At large distances from the Earth ($R > 1.5$ AU) the CIRs are bounded by two shocks, one at the leading antisolar edge (the forward shock) and a second at the trailing solar edge (the reverse shock). Figure 6 shows an interval during 1973 to 1974 where Pioneer 11 detected many CIRs and energetic ~ 0.5 to 1.8 MeV proton events. Figure 6 is taken from the “discovery paper” of shocks and energetic particles [Tsurutani *et al.*, 1982]. At CIR event “0” on day ~ 305 , there is a proton flux spike coincident with the CIR. However, at many CIRs (see events 1, 2, 3, 9, and 10) there are double spikes. These correspond to proton peaks at both the forward and reverse shocks. Typically higher fluxes are detected at the reverse shocks than at the forward shocks. It is speculated that it is the quasi-parallel nature of the reverse shocks that is the cause of this latter feature.

[24] The sequence of CIRs from events -3 to $+13$ occur at ~ 25 day intervals. This corresponds to the (equatorial) solar rotation period as seen by an observer (Pioneer 11) in inertial space. Note that in the ~ 0.5 to 1.8 MeV proton channel, there is no obvious flux “floor” or baseline. The inter-CIR proton intensities are highly variable.

[25] Why do we mention particle acceleration at $r > 1.5$ AU? These energetic particles can propagate back to 1 AU and can serve as part of the background flux at Earth. If these particles propagate even closer to the Sun, they can be accelerated by ICME shocks and become part of ESP events. We will discuss this topic again later in the paper.

2.6. Background Energetic Particles

[26] We have described SEPs coming from the solar flare sites, ESPs associated with ICME shocks and particles accelerated at CIR shocks. There are additional sources of the background particles as well. Galactic cosmic rays (GCRs) have the highest energies and are assumed to be created during supernova explosions or similar large-scale astrophysical events. The GCR intensities are modulated by solar activity as noted in Forbush decreases. The flux is minimum during solar maximum when the interplanetary magnetic field is the highest. These high fields “shield out” a portion of these particles. Anomalous cosmic rays (ACRs) have lesser energies than GCRs and are accelerated at the heliospheric termination shock. A description of these particles is included in Table 1.

2.7. Separation of Flare Photon and SEP and ESP Ionospheric Effects

[27] Energetic storm/prompt particles and solar energetic/delayed particles can cause ionization at Earth at the same time as the flare X-ray and EUV photons. This is apparent in Figure 1 where the three exist during the same (first) hour. How can one distinguish the effects of the different phenomena? The answer is: “with difficulty.” One could use particle spectra from near-Earth satellite data to model the ionospheric effects from the energetic particle precipitation and subtract that from the measured ionospheric

changes. Particle precipitation will also occur primarily in the magnetic polar regions and will occur at night as well as during the day.

[28] The initial part of the SFE is, however, purely due to solar photons. The reason for this is multifold. First, the energetic protons are typically nonrelativistic and are propagating at speeds far less than the speed of light. Second, owing to the curvature of the interplanetary magnetic field, the particles travel a longer distance than do the photons. It is estimated that the energetic particles travel at least ~ 1.3 to 1.4 AU to reach Earth distances. As a result, the flare electromagnetic emissions cause ionospheric effects first and they last for ~ 1 h. The flare EUV and X-ray emissions affect the dayside subsolar ionosphere. The SEP/ESP enhancements are delayed but can last for days or more. The SEPs/EPSSs affect the polar and high-latitude ionosphere over the whole globe. Therefore by studying the SFES on the dayside and nightside ionosphere, the effects due to SEPs/EPSSs can be distinguished from that of the electromagnetic component of the solar flare [Zhang and Xiao, 2005].

[29] What about relativistic electrons? Won't they reach the Earth rapidly and contaminate the flare photon effects? The acceleration of relativistic electrons at the flare site is often delayed from the flare by ~ 5 to 15 min [Hudson et al., 1982; Haggerty and Roelof, 2002]. This is in addition to propagation delays. This was the case for the 28 and 29 October 2003. There was no such a delay for the 14 July 2000 event. At this time there is not a good explanation for these delays or lack of delays. It is difficult to explain in a theoretical sense. However, it does offer modelers a way to partially separate the effects of flare photon phenomena from that of energetic particles.

2.8. Separation of SEP and Shock-Compression Ionospheric Effects

[30] Plasma densities increase downstream of fast forward shocks due to shock compression effects [Kennel et al., 1985]. The density increase ratios are roughly the magnetosonic Mach number values (up to a maximum of 4.0). Typical fast interplanetary shocks have Mach numbers of 2 to 3 [Tsurutani and Lin, 1985], thus the ram pressure increases by a factor of 2 to 3 across ICME shocks. Sudden compressions of the magnetosphere can cause dayside auroras [Zhou and Tsurutani, 1999; Tsurutani and Zhou, 2003] and trigger supersubstorms [Zhou and Tsurutani, 2004]. The dayside auroral precipitation will occur at auroral zone (60° – 65° MLAT) and middle latitudes on the dayside and the supersubstorm precipitation at auroral zone latitudes on the nightside. The energies of the precipitating particles are ~ 10 to 100 keV, so the enhanced ionization in the ionosphere will occur at altitudes of ~ 80 to 120 km. Shock compression can also lead to stable trapping of a portion of the SEP population that had entered the magnetosphere. This latter

effect will lead to the formation of a new radiation belt at low latitudes [Hudson et al., 1997, 2004; Looper et al., 2005]. Complicating these magnetospheric/ionospheric effects is that the SEP population is often the highest at and near the shock. These (untrapped) particles will also be entering the magnetosphere with some of them precipitating into the ionosphere (at all local times). A fourth energetic particle effect occurs if magnetic fields in the sheath region behind the shock or in the driver gas/ICME are southwardly directed. Magnetic reconnection will occur between the interplanetary fields and the magnetopause fields and a concomitant magnetic storm will result [Tsurutani et al., 1988; Gonzalez et al., 1994]. Large magnetic storms cause particle accumulation in the Earth magnetotail and magnetosphere, with subsequent energetic (~ 10 keV to ~ 1 MeV) particle precipitation at all local times. The precipitation will typically occur at middle latitudes, but during extreme storms, particles can be injected to latitudes as low as 45° .

[31] Details on interplanetary causes of middle-latitude ionospheric disturbances can be found in a review by Tsurutani et al. [2008a]. Ionospheric storms are discussed by Pröls [2004] and Mendillo [2006]. Wissing et al. [2008] have noted that signatures of SEP events and magnetic storms in electron fluxes are roughly comparable. The latter authors suggested that these two signatures can be separated based on Kp activity indices and energetic particle fluxes measured by EPAM instrument onboard ACE.

[32] There is another important connection between geomagnetic activity and SEP effects in the polar region ionosphere. The Earth's magnetic field shields against relatively low-energy particles (~ 10 – ~ 100 MeV) reaching middle latitudes due to geomagnetic cutoff effects. Magnetic reconnection during magnetic storms cause expansion of the auroral oval and the open field line region to lower latitudes, thus decreasing the geomagnetic cutoff latitude. Measurements made from the SAMPEX satellite during large SEP events [Leske et al., 2001] have shown that during storms the cutoff location was decreased by more than $\sim 5^\circ$.

2.9. Penetration of Interplanetary Electric Fields and Ionospheric Effects

[33] Sheath or ICME southward magnetic fields that create magnetic storms through a magnetic reconnection process also affect the \sim local noon and \sim local midnight equatorial ionospheres. The solar wind convection of southward magnetic fields past the magnetosphere represents a dawn-to-dusk interplanetary motional electric field. If a portion of this electric field enters the magnetosphere/ionosphere system (through magnetic reconnection or other processes), the electric field will uplift the equatorial ionosphere in the dayside and suppress it at night. At the noon equator, the ionosphere gets lifted to

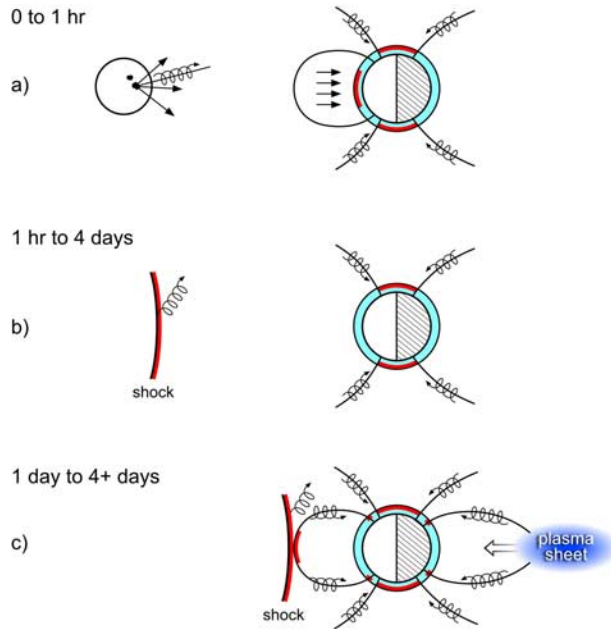


Figure 7. A schematic giving the time sequence of SFES on the ionosphere: (a) solar flare photon ionization of the subsolar dayside atmosphere. Flare particles precipitate into the polar atmosphere. (b) ICME shock particle acceleration and precipitation into the polar atmospheres. (c) ICME shock/sheath compression of the dayside magnetosphere causing dayside auroras, ICME sheath/MC southward magnetic fields cause magnetic storms.

higher altitudes where the recombination timescales are longer. Solar photoionization creates a new ionosphere at lower altitudes, increasing the overall TEC of the ionosphere. This is called a positive ionospheric storm. This interplanetary control of the dayside ionosphere has thus been called the “dayside ionospheric superfountain” or DIS [Tsurutani *et al.*, 2004, 2008b; Mannucci *et al.*, 2005, 2008; Verkhoglyadova *et al.*, 2006, 2008b] effect. At night, the electric field $E \times B$ convects the ionosphere to lower altitudes where chemical recombination takes place, reducing the TEC of the ionosphere. This is called a negative ionospheric storm.

3. Summary

[34] The number of photon and energetic particle effects on the Earth’s ionosphere is very large and can be confusing. For this reason we have constructed a time line and descriptive narrative of these effects to aid the reader.

[35] The time of occurrence of SFE effects are shown in Figure 7. Figure 7a shows the time interval from the flare

onset ($T = 0$) to ~ 1 h afterward. Flare photons travel directly from the flare site to the Earth, creating ionization in the dayside atmosphere/ionosphere primarily at the subsolar region. Generally, the more energetic photons cause ionization deeper in the atmosphere. The photons traverse the 1 AU distance in 8 min. Flares last from ~ 30 min to ~ 1 h, so the resultant ionization continues throughout the event. Owing to the thickness of the atmosphere and the grazing angle of incidence at the poles and the terminators, lesser ionization occurs in these regions than at the subsolar point.

[36] Flare energetic particles arrive shortly after the flare photons. The time delay depends on the particle’s kinetic energy, pitch angle, and magnetic connectivity. The particles enter the polar ionosphere. The more energetic particles penetrate deeper into the atmosphere.

[37] Another source of energetic particles is acceleration at a fast ICME shock illustrated in Figure 7b. ICME shocks first form at a distance of ~ 3 to 10 solar radii from the Sun [Tsurutani *et al.*, 2003b] and they propagate from their formation site to 1 AU and beyond. Since the transit time of a shock/ICME takes from 1 to 4 days to reach the Earth and energetic particles are continuously produced by this source, the Earth’s ionosphere is continuously bombarded by this precipitation. These particles will enter the polar ionospheric regions very much like the solar flare particles. They are somewhat less energetic than particles accelerated at the flare site however.

[38] When the high plasma densities behind the ICME shock (called the sheath) hit the magnetosphere, the resulting compression betatron accelerates magnetospheric 10–100 keV protons and electrons. Plasma instabilities lead to pitch angle scattering and the loss of these particles to the auroral zone and midlatitude dayside ionosphere. This is illustrated in Figure 7c. The shock/sheath compression can also trigger a supersubstorm in the Earth’s magnetotail. This will lead to energetic particle precipitation in the nightside auroral zone ionosphere.

[39] If the ICME sheath or ICME proper has southward directed magnetic fields, magnetic reconnection between the interplanetary magnetic fields and magnetopause fields will take place, leading to a magnetic storm. Because magnetic reconnection during a storm is much greater than during more normal conditions, the plasma is injected deeply into the magnetosphere. The particles are lost by scattering with a timescale of ~ 10 h. The particles precipitate into the middle latitude ionosphere at all local times.

[40] A third feature is shown in Figure 7c. As the ICME shock nears the magnetosphere, the particle fluxes at Earth become higher. During magnetic storms, the magnetic erosion is higher and the region of open flux larger. Therefore these energetic particles will have access to slightly lower latitudes. The polar regions may descend to 55° to 60° MLAT.

[41] Figure 7c also shows the effect of the interplanetary electric field. The dayside ionosphere is lifted to higher altitudes and the nightside ionosphere convected to lower altitudes.

4. Comments on Terminology

[42] The above terminology used by the solar, heliospheric, magnetospheric and ionospheric communities are confusing partly because the terms were developed many years ago by one community without regard to the terminology of others. This is a natural course in the initial phases of scientific development. However, as knowledge becomes greater and the cause/effect relationships become clearer, scientists should develop better (descriptive) terms. We have noted several conflicts in the usage of terms within this paper. Many heliospheric particle people use the term “energetic storm particle” (ESP) without reference to flares or to “solar storms” (the latter phrase is rarely used in context of flares). Magnetospheric and ionospheric scientists use the term “geomagnetic storm” or the shorter version “storm” to indicate a magnetospheric and ionospheric phenomenon. When the latter communities refer to “energetic storm particles,” they mean particles that have been accelerated within the magnetosphere, not those in interplanetary space. Thus for this reason we recommend changing the name ESP to SESP (solar energetic storm particles) or the other name “prompt particles.”

[43] The term SFE is also dated. We have indicated that there are a variety of “solar flare effects,” thus the term is vague. Solar flare photons have definite ionospheric effects. However, the solar flare-related prompt and delayed particles also affect the ionosphere. The effects of the latter are distinct and are of a different nature. We have also pointed out that there is a variable background of energetic particles in the heliosphere. These are presumably due to an amalgamation of prompt, delayed, CIR shock-related, planetary magnetosphere-related and anomalous cosmic ray particles that are propagating and scattering in the heliosphere. Some of the “prompt particles” initially accelerated at a solar flare site may travel through the heliosphere, eventually come back to the Sun and become part of the “energetic background.” If these particles are accelerated by an ICME shock (similar to CIR shock particles), these “prompt particles” could then precipitate into the ionosphere days or even months after the flare took place. Thus, even the term “prompt” can be ambiguous.

[44] The term SID is also ambiguous. It generally refers to the sudden increased dayside ionization associated with solar flares as discussed in this paper. However, ICME shock impingements on the dayside magnetosphere cause compressions of existing outer zone magnetospheric plasma, resultant plasma instabilities and sudden dayside

auroras and enhanced auroral zone ionization [Zhou and Tsurutani, 1999; Tsurutani et al., 2001; Zhou et al., 2003]. More specific terminology for SIDs could therefore be SIDF (sudden ionospheric disturbance flare) and SIDS (sudden ionospheric disturbance shock).

[45] Most of the older terminology mentioned in the paper are descriptive or phenomenological terms. They were originally developed when it was not certain what the physical causes for the phenomena were. As we develop greater understanding, it will be much more useful for researchers to develop and use physics-based terms.

[46] **Acknowledgments.** Portions of this work were performed at the Jet Propulsion Laboratory, California Institute of Technology, under contract with the National Aeronautics and Space Administration. G.S.L. thanks the Indian National Science Academy, New Delhi, for support under the Senior Scientist Scheme. O.P.V., G.L., and G.P.Z. acknowledge partial support of NASA grants NNG04GF83G, NNG05GH38G, and NNG05GM62G. The authors would like to thank A. Dmitriev, H. Hudson, M.-B. Kallenrode, R. A. Mewaldt, G. Pröls, and T. Woods for stimulating discussions and critical readings of the manuscript. We acknowledge the ACE ULEIS and SIS instrument teams and the ACE Science Center for providing the ACE data.

References

- Afraimovich, E. L. (2000), GPS global detection of the ionospheric response to solar flares, *Radio Sci.*, *35*, 1417, doi:10.1029/2000RS002340.
- Afraimovich, E. L., A. T. Altyntsev, V. V. Grechnev, and L. A. Leonovich (2002), The response of the ionosphere to faint and bright solar flares as deduced from global GPS network data, *Ann. Geophys.*, *45*, 31.
- Axford, W. I., E. Leer, and G. Skadron (1977), The acceleration of cosmic rays by shock waves, *Proc. Int. Conf. Cosmic Rays 15th*, *11*, 132.
- Bell, A. R. (1978), The acceleration of cosmic rays in shock fronts, I, *Mon. Not. R. Astron. Soc.*, *182*, 147.
- Carrington, R. C. (1860), Description of a singular appearance seen in the Sun on September 1, 1859, *Mon. Not. R. Astron. Soc.*, *XX*, 13.
- Cohen, R. H. (1976), Runaway electrons in an impure plasma, *Phys. Fluids*, *19*, 239, doi:10.1063/1.861451.
- Dmitriev, A. V., H.-C. Yeh, J.-K. Chao, I. S. Veselovsky, S.-Y. Su, and C. C. Fu (2006), Top-side ionosphere response to extreme solar events, *Ann. Geophys.*, *24*, 1469.
- Donnelly, R. F. (1976), Empirical models of solar flare x-ray and EUV emissions for use in studying their E and F region effects, *J. Geophys. Res.*, *81*, 4745, doi:10.1029/JA081i025p04745.
- Fermi, E. (1950), *Nuclear Physics*, pp. 30 and 215, Univ. of Chicago Press, Chicago, Ill.
- Feynman, J., and S. B. Gabriel (2000), On space weather consequences and predictions, *J. Geophys. Res.*, *105*(A5), 10,543, doi:10.1029/1999JA000141.

- Gonzalez, W. D., J. A. Joselyn, Y. Kamide, H. W. Kroehl, G. Rostoker, B. T. Tsurutani, and V. M. Vasyliunas (1994), What is a geomagnetic storm?, *J. Geophys. Res.*, *99*, 5771, doi:10.1029/93JA02867.
- Haggerty, D. K., and E. C. Roelof (2002), Impulsive near-relativistic solar electron events: Delayed injection with respect to solar electromagnetic emissions, *Astrophys. J.*, *579*, 841, doi:10.1086/342870.
- Hudson, H. S., R. P. Lin, and R. T. Stewart (1982), Second-stage acceleration in a limb-occulted flare, *Sol. Phys.*, *75*, 245, doi:10.1007/BF00153475.
- Hudson, M. K., S. R. Elkington, J. G. Lyon, V. A. Marchenko, I. Roth, M. Temerin, J. B. Blake, M. S. Gussenhoven, and J. R. Wygant (1997), Simulations of radiation belt formation during storm sudden commencements, *J. Geophys. Res.*, *102*, 12,087, doi:10.1029/97JA03995.
- Hudson, M. K., B. T. Kress, J. E. Mazur, K. L. Perry, and P. L. Slocum (2004), 3D modeling of shock-induced trapping of solar energetic particles in the Earth's magnetosphere, *J. Atmos. Sol. Terr. Phys.*, *66*, 1389, doi:10.1016/j.jastp.2004.03.024.
- Judge, D. L. (1998), First solar EUV irradiance obtained from SOHO by the CELIAS/SEM, *Sol. Phys.*, *177*, 161, doi:10.1023/A:1004929011427.
- Kallenrode, M.-B. (2001), *Space Physics: An Introduction to Plasmas and Particles in the Heliosphere and Magnetospheres*, Springer, New York.
- Kallenrode, M.-B. (2003), Current views on impulsive and gradual solar energetic particle events, *J. Phys. G Nucl. Part. Phys.*, *29*, 965, doi:10.1088/0954-3899/29/5/316.
- Kennel, C. F., J. P. Edmiston, and T. Hada (1985), A quarter century of collisionless shock research, in *Collisionless Shocks in the Heliosphere: A Tutorial Review*, *Geophys. Monogr. Ser.*, vol. 34, edited by R. G. Stone and B. T. Tsurutani, AGU, Washington, D. C.
- Klobuchar, J. A. (1997), Real-time ionospheric science: The new reality, *Radio Sci.*, *32*(5), 1943–1952, doi:10.1029/97RS01234.
- Leonovich, L. A., E. L. Afraimovich, E. B. Romanova, and A. V. Tschillin (2002), Estimating the contribution from different ionospheric regions to the TEC response to the solar flares using data from the international GPS network, *Ann. Geophys.*, *20*, 1935.
- Leske, R. A., R. A. Mewaldt, E. C. Stone, and T. T. von Rosenvinge (2001), Observations of geomagnetic cutoff variations during solar energetic particle events and implications for the radiation environment at the Space Station, *J. Geophys. Res.*, *106*(A12), 30,011–30,022, doi:10.1029/2000JA000212.
- Li, G., and G. P. Zank (2005), Mixed particle acceleration at CME-driven shocks and flares, *Geophys. Res. Lett.*, *32*, L02101, doi:10.1029/2004GL021250.
- Li, G., G. P. Zank, and W. K. M. Rice (2003), Energetic particle acceleration and transport at coronal mass ejection-driven shocks, *J. Geophys. Res.*, *108*(A2), 1082, doi:10.1029/2002JA009666.
- Li, G., G. P. Zank, and W. K. M. Rice (2005), Acceleration and transport of heavy ions at coronal mass ejection-driven shocks, *J. Geophys. Res.*, *110*, A06104, doi:10.1029/2004JA010600.
- Litvinenko, Y. E. (2003), Energies of electrons accelerated in turbulent reconnection current sheets in solar flares, *Sol. Phys.*, *212*, 379, doi:10.1023/A:1022942923783.
- Looper, M. D., J. B. Blake, and R. A. Mewaldt (2005), Response of the inner radiation belt to the violent Sun-Earth connection events of October–November 2003, *Geophys. Res. Lett.*, *32*, L03S06, doi:10.1029/2004GL021502.
- Mannucci, A. J., B. T. Tsurutani, B. A. Iijima, A. Komjathy, A. Saito, W. D. Gonzalez, F. L. Guarnieri, J. U. Kozyra, and R. Skoug (2005), Dayside global ionospheric response to the major interplanetary events of October 29–30 2003 “Halloween storms”, *Geophys. Res. Lett.*, *32*, L12S02, doi:10.1029/2004GL021467.
- Mannucci, A. J., B. T. Tsurutani, M. A. Abdu, W. D. Gonzalez, A. Komjathy, E. Echer, B. A. Iijima, G. Crowley, and D. Anderson (2008), Superposed epoch analysis of the dayside ionospheric response to four intense geomagnetic storms, *J. Geophys. Res.*, *113*, A00A02, doi:10.1029/2007JA012732.
- Mendillo, M. (2006), Storms in the ionosphere: Patterns and processes for total electron content, *Rev. Geophys.*, *44*, RG4001, doi:10.1029/2005RG000193.
- Miller, J. A., T. N. LaRosa, and R. L. Moore (1996), Stochastic electron acceleration by cascading fast mode waves in impulsive solar flares, *Astrophys. J.*, *461*, 445, doi:10.1086/177072.
- Mitra, A. P. (1974), *Ionospheric Effects of Solar Flares*, Springer, New York.
- Pröls, G. (2004), *Physics of the Earth's Space Environment*, Springer, Heidelberg, Germany.
- Rohen, G., et al. (2005), Ozone depletion during the solar proton events of October/November 2003 as seen by SCIAMACHY, *J. Geophys. Res.*, *110*, A09S39, doi:10.1029/2004JA010984.
- Sahai, Y., F. Becker-Guedes, P. R. Fagundes, W. L. C. Lima, A. J. de Abreu, F. L. Guarnieri, C. M. N. Candido, and V. G. Pillat (2006), Unusual ionospheric effects observed during the intense 28 October 2003 solar flare in the Brazilian sector, *Ann. Geophys.*, *25*, 2497.
- Thome, G. D., and L. S. Wagner (1971), Electron density enhancements in the E and F regions of the ionosphere during solar flares, *J. Geophys. Res.*, *76*, 6883, doi:10.1029/JA076i028p06883.
- Thomson, N. R., C. J. Rodger, and R. L. Dowden (2004), Ionosphere gives the size of the greatest solar flare, *Geophys. Res. Lett.*, *31*, L06803, doi:10.1029/2003GL019345.
- Tsurutani, B. T., and R. P. Lin (1985), Acceleration of >47 keV ions and >2 keV electrons by interplanetary shocks at 1 AU, *J. Geophys. Res.*, *90*, 1, doi:10.1029/JA090iA01p00001.
- Tsurutani, B. T., and X. Y. Zhou (2003), Interplanetary shock triggering of substorms: WIND and Polar, *Adv. Space Res.*, *31*, 1063, doi:10.1016/S0273-1177(02)00796-2.

- Tsurutani, B. T., E. J. Smith, K. R. Pyle, and J. A. Simpson (1982), Energetic protons accelerated at corotating shocks: Pioneer 10 and 11 observations from 1 to 5 AU, *J. Geophys. Res.*, *87*, 7389, doi:10.1029/JA087iA09p07389.
- Tsurutani, B. T., W. D. Gonzalez, F. Tang, S.-I. Akasofu, and E. J. Smith (1988), Origin of interplanetary southward magnetic fields responsible for major magnetic storms near solar maximum (1978–1979), *J. Geophys. Res.*, *93*, 8519, doi:10.1029/JA093iA08p08519.
- Tsurutani, B. T., X.-Y. Zhou, V. M. Vasyliunas, G. Haerendel, J. K. Arballo, and G. S. Lakhina (2001), Interplanetary shocks, magnetopause boundary layers and dayside auroras: The importance of a very small magnetospheric region, *Surv. Geophys.*, *22*, 101, doi:10.1023/A:1012952414384.
- Tsurutani, B. T., W. D. Gonzalez, G. S. Lakhina, and S. Alex (2003a), The extreme magnetic storm of 1–2 September 1859, *J. Geophys. Res.*, *108*(A7), 1268, doi:10.1029/2002JA009504.
- Tsurutani, B., S. T. Wu, T. X. Zhang, and M. Dryer (2003b), Coronal mass ejection (CME)-induced shock formation, propagation and some temporally and spatially developing shock parameters relevant to particle energization, *Astron. Astrophys.*, *412*, 293.
- Tsurutani, B. T., et al. (2004), Global dayside ionospheric uplift and enhancement associated with interplanetary electric fields, *J. Geophys. Res.*, *109*, A08302, doi:10.1029/2003JA010342.
- Tsurutani, B. T., et al. (2005), The October 28, 2003 extreme EUV solar flare and resultant extreme ionospheric effects: Comparison to other Halloween events and the Bastille day event, *Geophys. Res. Lett.*, *32*, L03S09, doi:10.1029/2004GL021475.
- Tsurutani, B. T., et al. (2006), Extreme solar EUV flares and ICMEs and resultant extreme ionospheric effects: Comparison of the Halloween 2003 and the Bastille day events, *Radio Sci.*, *41*, RS5S07, doi:10.1029/2005RS003331.
- Tsurutani, B. T., E. Echer, F. Guarnieri, and O. P. Verkhoglyadova (2008a), in *Midlatitude Ionospheric Dynamics and Disturbances*, *Geophys. Monogr. Ser.*, vol. 181, edited by P. Kintner et al., AGU, Washington, D. C.
- Tsurutani, B. T., et al. (2008b), Prompt penetration electric fields (PPEFs) and their ionospheric effects during the great magnetic storm of 30–31 October 2003, *J. Geophys. Res.*, *113*, A05311, doi:10.1029/2007JA012879.
- Verkhoglyadova, O. P., B. T. Tsurutani, and A. J. Mannucci (2006), Temporal development of dayside TEC variations during the October 30, 2003 superstorm: Matching modeling to observations, in *Solar Terrestrial (ST) 2007*, *Adv. Geosci.*, vol. 11, edited by M. Duldig et al., World Sci. Publ., Singapore.
- Verkhoglyadova, O. P., G. Li, G. P. Zank, and Q. Hu (2008a), Modeling a mixed SEP event with the PATH model: December 13, 2006, in *Particle Acceleration and Transport in the Heliosphere and Beyond: 7th Annual International Astrophysics Conference*, *AIP Conf. Proc.*, *1039*, 214, doi:10.1063/1.2982448.
- Verkhoglyadova, O. P., B. T. Tsurutani, A. J. Mannucci, A. Saito, T. Araki, D. Anderson, M. Abdu, and J. H. A. Sobral (2008b), Simulation of PPEF effects in dayside low-latitude ionosphere for the October 30, 2003 superstorm, in *Midlatitude Ionospheric Dynamics and Disturbances*, *Geophys. Monogr. Ser.*, vol. 181, edited by P. Kintner et al., AGU, Washington, D. C.
- Verkhoglyadova, O. P., G. Li, G. P. Zank, and Q. Hu (2009), Using the PATH code for modeling gradual SEP events in the inner heliosphere, *Astrophys. J.*, *693*, 894, doi:10.1088/0004-637X/693/1/894.
- Wissing, J. M., J. P. Bornebusch, and M.-B. Kallenrode (2008), Variation of energetic particle precipitation with local magnetic time, *Adv. Space Res.*, *41*, 1274, doi:10.1016/j.asr.2007.05.063.
- Woods, T. N., F. G. Eparvier, J. Fontenla, J. Harder, G. Kopp, W. E. McClintock, G. Rottman, B. Smiley, and M. Snow (2004), Solar irradiance variability during the October 2003 solar storm period, *Geophys. Res. Lett.*, *31*, L10802, doi:10.1029/2004GL019571.
- Woods, T. N., G. Kopp, and P. C. Chamberlin (2006a), Contributions of the solar ultraviolet to the total solar irradiance during large flares, *J. Geophys. Res.*, *111*, A10S14, doi:10.1029/2005JA011507.
- Woods, T. N., J. L. Lean, and F. G. Eparvier (2006b), The EUV Variability Experiment (EVE): Science plans and instrument overview, in *Proceedings of International Living With a Star (ILWS)*, edited by N. Gopalswamy and A. Bhattacharyya, Quest Publ., Goa, India.
- Zank, G. P., W. K. M. Rice, and C. C. Wu (2000), Particle acceleration and coronal mass ejection driven shocks: A theoretical model, *J. Geophys. Res.*, *105*(A11), 25,079, doi:10.1029/1999JA000455.
- Zank, G. P., G. Li, and O. P. Verkhoglyadova (2007), Particle acceleration at interplanetary shocks, *Space Sci. Rev.*, *130*, 255, doi:10.1007/s11214-007-9214-2.
- Zhang, D. H., and Z. Xiao (2003), Study of the ionospheric total electron content response to the great flare on 15 April 2001 using the International GPS Service network for the whole sunlit hemisphere, *J. Geophys. Res.*, *108*(A8), 1330, doi:10.1029/2002JA009822.
- Zhang, D. H., and Z. Xiao (2005), Study of ionospheric response to the 4B flare on 28 October 2003 using International GPS Service network data, *J. Geophys. Res.*, *110*, A03307, doi:10.1029/2004JA010738.
- Zhang, D. H., Z. Xiao, K. Igarashi, and G. Y. Ma (2002), GPS-derived ionospheric total electron content response to a solar flare that occurred on 14 July 2000, *Radio Sci.*, *37*(5), 1086, doi:10.1029/2001RS002542.
- Zhou, X.-Y., and B. T. Tsurutani (1999), Rapid intensification and propagation of the dayside aurora: Large scale interplanetary pressure pulses (fast shocks), *Geophys. Res. Lett.*, *26*, 1097, doi:10.1029/1999GL900173.
- Zhou, X.-Y., and B. T. Tsurutani (2004), Dawn and dusk auroras caused by gradual, intense solar wind ram pressure events,

- J. Atmos. Sol. Terr. Phys.*, 66, 153, doi:10.1016/j.jastp.2003.09.008.
- Zhou, X.-Y., R. J. Strangeway, P. C. Anderson, D. G. Sibeck, B. T. Tsurutani, G. Haerendel, H. U. Frey, and J. K. Arballo (2003), Shock aurora: FAST and DMSP observations, *J. Geophys. Res.*, 108(A4), 8019, doi:10.1029/2002JA009701.
-
- G. S. Lakhina, Indian Institute of Geomagnetism, New Panvel (W), Navi Mumbai 410218, India.
- G. Li and G. P. Zank, CSPAR, University of Alabama, Huntsville, AL 92521, USA.
- A. J. Mannucci, B. T. Tsurutani, and O. P. Verkhoglyadova, Jet Propulsion Laboratory, California Institute of Technology, Pasadena, CA 91109, USA. (bruce.t.tsurutani@jpl.nasa.gov)